measured by using a saturation recovery method with a variable repetition time (TR) SE imaging sequence (16): TR 600, 1000, 2000, 4000, 8000 ms; echo time (TE) 10 ms; bandwidth (BW) 16 kHz; field of view (FOV) 40 × 30 mm; matrix size 256 × 160; slice thickness 1 mm; slice gap 1 mm; number of slices 16; number of excitations (NEX) 1; coronal plane. An 8-cm polyvinyl chloride tube with an outer diameter of 2.7 mm was inserted into the animal's trachea, and the rats were ventilated with an average of 2–3 ml per breath of a mixture of O_2, N_2, and air (2:1:10) using a small animal ventilator (CWE SAR-830/AP Ventilator; CWE, Inc., Ardmore, Pa., USA) at an average of 80 breaths per minute. Body temperature was monitored rectally (36.0 ± 0.5℃).

T1 values were estimated on a pixel-by-pixel basis using the non-linear least-square fit of the signal intensity measured for each TR value. In the obtained T1 images, regions of interest (ROIs) were placed on the thalamus, hippocampus, olfactory bulb, cerebral cortex, corpus callosum, midbrain, cerebellum, pons, cerebrospinal fluid, and muscle. Mean T1 values were calculated from each ROI. A mean and a standard deviation of the mean values obtained from three rats were calculated.

Phantom study

Phantom preparation. Gd-DTPA (Magnevist; Bayer Schering Pharma, Osaka, Japan) was diluted with saline to obtain 19 solutions with different concentrations (0, 0.01, 0.03, 0.05, 0.07, 0.1, 0.15, 0.2, 0.25, 0.3, 0.5, 0.7, 1, 3, 5, 7, 10, 30, and 50 mM). Each solution was encapsulated in separate polypropylene vials with a diameter of 27 mm, which were set in agar.

T1 measurement. T1 values of each Gd-DTPA solution were measured at room temperature using the same pulse sequence as the T1 measurement in normal rats: TR 34, 100, 200, 400, 600, 800, 1000, 1200, 1400, 1600, 1800, 2000, 4000, 6000, 8000, 11,000, 15,000 ms; TE 9 ms; BW 16 kHz; FOV 210 × 158 mm; matrix size 256 × 192; slice thickness 3 mm; number of slices 1; NEX 1. A standard quadrature birdcage head coil was used.

Circular ROIs with 70–80% of the diameter of a vial were placed on a homogeneous signal portion of each phantom image. T1 values were estimated by non-linear least-square fit of the average signal intensity of all voxels in the ROI measured for each TR value. Five measurements were performed for phantoms, and the mean and standard deviation of measured T1 values were calculated.

Choice of pulse sequences. We used a Gd-DTPA saline solution (0.1 mM) with a T1 value close to that in the normal thalamus as a corresponding solution to the glioma in the thalamus region before contrast. We hypothesized that T1 in the glioma would not be so different from that in normal tissue. Saline solutions with a higher concentration of Gd-DTPA were regarded as a corresponding solution to the glioma after contrast.

T1W images of each phantom were acquired at room temperature (approximately 21℃) using four clinically available pulse sequences (SE, fast SE [FSE], IR-FSE [T1FLAIR], and fast spoiled GRE [FSPGR]) (Table 1). A standard quadrature birdcage head coil was used for the imaging of phantoms.

Circular ROIs with 70–80% of the diameter of the vial were placed on a uniform signal portion of each phantom. Mean signal intensities were calculated from each ROI. For each sequence, signal enhancements of each Gd-DTPA solution (E_P) were calculated as $E_P = S/S_0$, where S is the signal intensity of each solution and S_0 is that of 0.1 mM of the solution. The pulse sequences showing high E_P were used for the imaging of C6 glioma model rats and were compared based on Gd-DTPA-induced signal enhancements in brain tumors, delineated by histopathology.

Rat brain C6 glioma model study

Preparation of rat brain C6 glioma models. C6 glioma cells (CCL-107 cell line, ATCC; Summit Pharmaceuticals International Corporation, Tokyo,

Table 1. Pulse sequences and imaging parameters used for imaging of saline phantoms containing gadopentetate dimeglumine (Gd-DTPA)

Pulse sequence	TR, ms	TE, ms	TI, ms	FA, °	ETL	BW, kHz	NEX	Acquisition time, min:s
SE	1400	14	—	—	—	16	1	4:46
FSE	1400	16	—	—	3	32	1	1:52
T1FLAIR	3000	16	1300	—	3	32	1	4:00
FSPGR	20	3.2	—	30	—	32	10	0:39

For all pulse sequences, FOV was 210 × 158 mm, matrix was 256 × 192, the number of slices was 1, and the slice thickness was 3 mm. SE: spin echo; FSE: fast spin echo; T1FLAIR: inversion recovery fast spin echo; FSPGR: fast spoiled gradient echo; TR: repetition time; TE: echo time; TI: inversion time; FA: flip angle; ETL: echo train length; BW: bandwidth; NEX: number of excitations.

Acta Radiologica rad134548.3d 23/10/07 20:33:24
The Charlesworth Group, Wakefield +44(0)1924 369598 - Rev 7.51n/W (Jan 20 2003)

262880

Japan) were implanted into the region of the thalamus in the left hemispheres of the brains of 20 rats (8 weeks old, 292.8±14.8 g). The implantation procedures were performed under general anesthesia using an intramuscular injection of ketamine (33 mg/kg; Sankyo Co., Ltd., Tokyo, Japan) and xylazine (7 mg/kg; Bayer AG, Leverkusen, Germany). A burr hole was made 3 mm lateral and 2 mm posterior to the bregma using a dental drill. A needle with an outer diameter of 0.3 mm was inserted 4 mm below the outer table of the skull through the burr hole. A 10-μl solution containing 10^7 cells/ml was infused over 5 min at a constant rate using a microsyringe (Hamilton Co., Reno, Nev., USA) and infusion pump (Eicom Corp., Kyoto, Japan).

MR imaging. Two weeks after implantation, all 20 rats underwent screening by T1W imaging after Gd-DTPA administration. Developed glioma was confirmed in only five out of 20 rats. Those five rats were used for experiments for the comparison of pulse sequences. Three weeks after implantation, when the glioma was fully developed, T1W brain images of the selected five rats (11 weeks old, 301.3±29.0 g) were acquired before and after Gd-DTPA administration using three pulse sequences determined by the phantom study (Table 2) in the coronal plane. Rats were given general anesthesia with an intramuscular injection of a ketamine (33 mg/kg) and xylazine (7 mg/kg) mixture, and allowed to breathe spontaneously during preparation and imaging. First, precontrast T1W images were acquired. Then, a dose of 0.1 mmol/kg of Gd-DTPA was administered by hand injection followed by a 3.0-ml saline flush through a 22G indwelling needle placed in a tail or femoral vein. Postcontrast T1W imaging started 1 min after Gd-DTPA administration with identical settings to the precontrast imaging. Each rat was examined using all three pulse sequences (Table 2). In order to eliminate the effect of previously administered Gd-DTPA, three scans using different pulse sequences were performed on three separate days, at 22- to 26-hour intervals, in a randomized order.

ROI analysis. Based on the results of histopathology (see below), ROIs were placed on a portion of each glioma. Areas of necrosis or hemorrhage were excluded from the ROI. Mean signal intensities in the pre- and postcontrast T1W images were calculated from each ROI. For each sequence, signal enhancement of each glioma (E_T) was calculated as $E_T = S_{post}/S_{pre}$, where S_{post} is signal intensity in the glioma after contrast and S_{pre} is that before contrast.

Histopathology

One day after MR imaging, rat brains were removed and fixed in formalin. All brains were completely coronally sectioned. Sections were stained with hematoxylin and eosin (HE) in order to delineate areas of glioma, hemorrhage, and necrosis.

Statistical analysis

All parameters assessed were given as means ± standard deviations. Pair-wise comparison among pulse sequences was performed using the Tukey-Kramer test. A P value of <0.05 was considered statistically significant.

Results

T1 in normal rat brains

Fig. 2 shows images from one of the three normal rats used to quantitate T1 values in the brain. Table 3 summarizes the T1 values of typical brain structures. The T1 value in the thalamus was 1405±32 ms.

T1 of Gd-DTPA solutions

Fig. 3 shows selected images from a series of 17 images obtained with different TR values. Table 4 summarizes T1 values in the Gd-DTPA solutions

Table 2. Pulse sequences and imaging parameters used for imaging of rat brains with C6 glioma cell implants

Pulse sequence	TR, ms	TE, ms	FA, °	ETL	BW, kHz	NEX	Acquisition time, min:s
SE	1400	13	—	—	16	1	4:46
FSE	1400	18.6	—	3	32	3	4:32
FSPGR	20	4.7	30	—	32	8	5:40

For all pulse sequences, FOV was 60×45 mm, matrix was 256×192, the number of slices was 11, and the slice thickness was 2.5 mm (0.5-mm gap). SE: spin echo; FSE: fast spin echo; FSPGR: fast spoiled gradient echo; TR: repetition time; TE: echo time; FA: flip angle; ETL: echo train length; BW: bandwidth; NEX: number of excitations.

Acta Radiologica rad134548.3d 23/10/07 20:33:24
The Charlesworth Group, Wakefield +44(0)1924 369598 - Rev 7.51n/W (Jan 20 2003)

262880

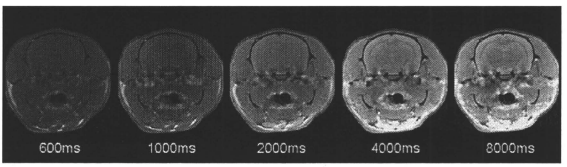

Fig. 2. Images from one of three rats used for the measurement of T1 values in normal rat brain. One of 16 slices acquired is shown. The images are arranged from left to right in ascending order of repetition time. All five images are set with equal window width and equal window level.

Table 3. T1 relaxation time in normal rat brain at 3T

	T1, ms
Thalamus	1405±32
Hippocampus	1779±151
Olfactory bulb	1613±117
Cerebral cortex	1506±13
Corpus callosum	1389±43
Midbrain	1329±50
Cerebellum	1726±356
Pons	1343±80
Cerebrospinal fluid	3460±737
Muscle	1529±99

Mean and standard deviation of values obtained from three rats.

ranging from 0 to 10 mM. In 30 and 50 mM solutions, an accurate T1 value could not be measured because of extensive signal loss due to T2 decay. The 0.1-mM solution showed a T1 value (1302±54 ms) closest to that in the normal thalamus (1405±32 ms).

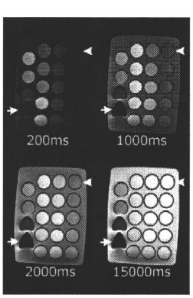

Fig. 3. Images obtained in the measurement of T1 values of 19 saline solutions with different concentrations of gadopentetate dimeglumine (0, 0.01, 0.03, 0.05, 0.07, 0.1, 0.15, 0.2, 0.25, 0.3, 0.5, 0.7, 1, 3, 5, 7, 10, 30, and 50 mM). The four selected images from a series of 17 images obtained with different TR values are shown. Each solution was encapsulated in separate polypropylene vials, which were set in agar. The concentration of gadopentetate dimeglumine decreases from bottom to top and from left to right. Arrows and arrowheads denote the 50-mM and 0-mM solutions, respectively. All four images are set with equal window width and equal window level.

Table 4. T1 of saline with different concentrations of Gd-DTPA at 3T

Gd-DTPA concentration, mM	T1, ms
0	3026±121
0.01	2652±96
0.03	2245±108
0.05	1970±92
0.07	1775±103
0.1	1302±54
0.15	993±57
0.2	820±52
0.25	737±51
0.3	666±63
0.5	389±17
0.7	284±12
1	209±9
3	84±4
5	58±2
7	36±1
10	27±1
30	—
50	—

Mean and standard deviation of values obtained from five measurements.

Choice of pulse sequences

Fig. 4 shows E_P in the Gd-DTPA solutions ranging from 0.1 to 50 mM. In Gd-DTPA solutions ranging from 0.15 to 30 mM, a higher E_P was obtained as follows: FSPGR > SE > FSE > T1FLAIR. Because E_P for T1FLAIR was lowest at all concentrations, T1FLAIR was not used for the imaging of rat brain tumors.

Based on our preliminary experiments, the T1 value in the glioma in the thalamus region after contrast was about 90% of that before contrast. Therefore, we regarded the 0.15-mM solution as a corresponding solution to glioma after contrast, and compared E_P values at 0.15 mM obtained using different sequences (Fig. 5). E_P at 0.15 mM was 1.10±0.02 for FSE, 1.16±0.01 for FSPGR, 1.16±0.01 for SE, and 1.06±0.01 for T1FLAIR. The Tukey-Kramer test showed significant differences ($P<0.05$) between all pairs except for FSPGR–SE. E_P for FSPGR was significantly higher than that for FSE and T1FLAIR and comparable to that for SE.

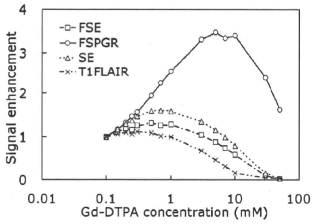

Fig. 4. Signal enhancements in saline solutions containing gadopentetate dimeglumine (Gd-DTPA) obtained by the following pulse sequences: spin echo (SE); fast spin echo (FSE); inversion recovery fast spin echo (T1FLAIR); fast spoiled gradient echo (FSPGR). Signal enhancement was the signal intensity scaled by that of a 0.1-mM Gd-DTPA solution whose T1 value was closest to the average T1 value in the brain parenchyma of normal rats.

Signal enhancement in rat brain C6 glioma

Fig. 6 displays typical pre- and postcontrast T1W images of brains of C6 glioma model rats, together with an example of ROIs placed on the glioma and HE-stained slices. Fig. 7 shows the comparison between E_T values for FSE, SE, and FSPGR. E_T values were 1.12 ± 0.05 for FSE, 1.26 ± 0.11 for FSPGR, and 1.20 ± 0.11 for SE. The Tukey-Kramer test showed the significant superiority of FSPGR over FSE. There was no significant difference between FSPGR and SE.

Discussion

T1W imaging using SE results in a corresponding restriction in the number of slices as a result of the

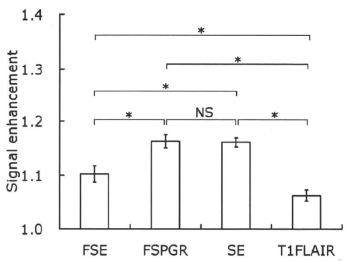

Fig. 5. Signal enhancement of saline solution with 0.15 mM Gd-DTPA obtained using different pulse sequences: spin echo (SE); fast spin echo (FSE); inversion recovery fast spin echo (T1FLAIR); fast spoiled gradient echo (FSPGR). Signal enhancement was defined as the signal intensity of a 0.15-mM solution scaled by that of a 0.1-mM solution. The Tukey-Kramer test was performed for pair-wise comparison among four pulse sequences. The asterisk and NS denote significant difference ($P < 0.05$) and no significant difference ($P > 0.05$), respectively.

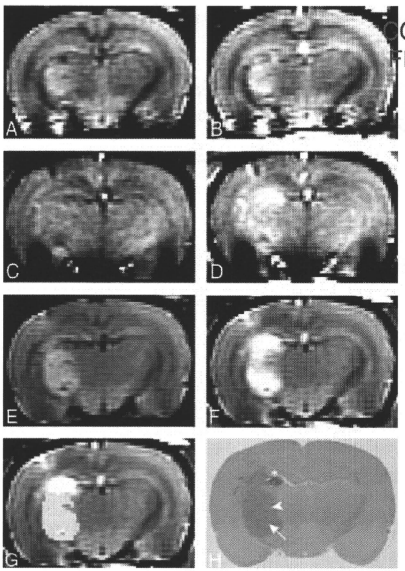

Fig. 6. Examples of pre- (A, C, E) and post-contrast (B, D, F) coronal T1-weighted images obtained using fast spin-echo (FSE) (A, B), fast spoiled gradient-echo (FSPGR) (C, D), and spin-echo (SE) (E, F) sequences. A region of interest (ROI) placed on the glioma (G) and a slice stained using hematoxylin and eosin (HE) (H). T1-weighted images were acquired 3 weeks after the implantation of C6 glioma cells. Areas of necrosis or hemorrhage, which were delineated based on histopathology, were excluded from ROIs. In the HE-stained slice, small-cell glioma (arrowhead), hemorrhage (asterisk), and necrosis (arrow) were found.

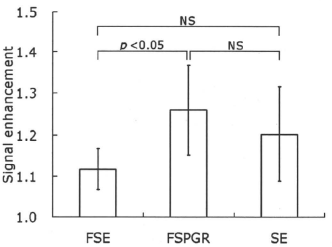

Fig. 7. Signal enhancement in rat brain C6 glioma obtained with different pulse sequences: spin echo (SE); fast spin echo (FSE); fast spoiled gradient echo (FSPGR). Signal enhancement was defined as the signal intensity after Gd-DTPA administration scaled by that before administration. The pair-wise comparison among pulse sequences was performed using the Tukey-Kramer test. NS denotes no significant difference ($P > 0.05$).

specific absorption rate (SAR) at 3T. The use of FSE makes radiofrequency heating more serious. Compared to SE and FSE, FSPGR provides relatively low radiofrequency heating and, if the NEX of FSPGR can be reduced, relatively short acquisition time. This depends on the signal-to-noise ratio, and we thought it possible based on our rat brain images (Fig. 6). Therefore, we examined the characteristics of signal enhancement in FSPGR. FSPGR provided significantly higher signal enhancement than FSE and comparable signal enhancement to SE, both in the 0.15-mM Gd-DTPA solution and in rat brain C6 glioma in the thalamus region. We speculate that FSPGR may be superior to FSE and comparable to SE in its ability to delineate brain tumors, although, in order to verify this speculation, several studies would be required using different cell types and various transplantation sites. Considering the advantage of FSPGR in terms of acquisition time and SAR limit, FSPGR may be more suitable for contrast-enhanced T1W imaging of brain tumors in clinical 3T scanners than SE. Additionally, high-resolution 3D images can be obtained by using FSPGR with a reasonable acquisition time so that small lesions may be better visualized. On the other hand, FSPGR was more sensitive to magnetic susceptibility artifacts than SE (Fig. 6). SE could therefore be more suitable than FSPGR for delineation of tumors in regions with susceptibility artifacts, such as the base of the skull.

E_T values obtained in our study (1.26 for FSPGR, 1.20 for SE, and 1.12 for FSE) were lower compared to previously reported values (1, 4, 5, 12). For example, RUNGE et al. reported that the E_T induced by Gd-DTPA was approximately 1.44 using SE in rat brain C6/LacZ glioma models at 3T (5). The difference between E_T in our study and that in previous reports may result from the difference in the type of tumor, in the degree of growth of brain tumors, or in TR. In our study, TR was adjusted to increase T1 contrast in the normal brain region for specification of more exact location of the glioma. Although the use of a shorter TR may increase signal enhancement in the glioma, contrast in the normal region would become unclear, and therefore it could become difficult to specify the location of the glioma exactly. Therefore, we used a longer TR than that in previous reports.

FISCHBACH et al. showed higher contrast in SE in patients, but they optimized the TR (600 ms) of SE by phantom experiments using a saline solution with a low concentration of Gd-DTPA (0.125 μM) (12), whose T1 is extremely long compared to that in the brain. We quantified T1 in rat brains and chose a proper TR (1400 ms) of SE to enhance normal brain contrast. Therefore, our comparison would be fairer and our results may be more closely extrapolated to human tumors.

One limitation of our work is our limited sample size. Although C6 glioma cells were implanted into 20 rats in our in-vivo study, only five rats could be used for the experiment, as C6 gliomas showed considerable individual variation in their growth and were fully developed only in five rats. Therefore, the number of test animals was relatively small, resulting in large standard deviations for E_T. A larger sample size may show a significant difference between FSPGR and SE.

In conclusion, FSPGR is superior to FSE and comparable to SE in its ability to delineate rat brain C6 glioma in the thalamus region using venous injection of Gd-DTPA.

Acknowledgments

This study was supported by a research grant on Advanced Medical Technology from the Ministry of Health, Labor and Welfare (MHLW), Japan (H17-nano-15), and a Program for Promotion of Fundamental Studies in Health Science of the Organization for Pharmaceutical Safety and Research (of Japan) Health Science Research Grant (H13-005) from the Ministry of Health, Labor and Welfare, (of Japan)

References

1. Nöbauer-Huhmann IM, Ba-Ssalamah A, Mlynarik V, Barth M, Schoggl A, Heimberger K, et al. Magnetic resonance imaging contrast enhancement of brain tumors at 3 tesla versus 1.5 tesla. Invest Radiol 2002;37:114–9.
2. Trattnig S, Ba-Ssalamah A, Noebauer-Huhmann IM, Barth M, Wolfsberger S, Pinker K, et al. MR contrast agent at high-field MRI (3 Tesla). Top Magn Reson Imaging 2003;14:365–75.
3. Ba-Ssalamah A, Nöbauer-Huhmann IM, Pinker K, Schibany N, Prokesch R, Mehrain S, et al. Effect of contrast dose and field strength in the magnetic resonance detection of brain metastases. Invest Radiol 2003;38:415–22.
4. Biswas J, Nelson CB, Runge VM, Wintersperger BJ, Baumann SS, Jackson CB, et al. Brain tumor enhancement in magnetic resonance imaging: comparison of signal-to-noise ratio (SNR) and contrast-to-noise ratio (CNR) at 1.5 versus 3 tesla. Invest Radiol 2005;40: 792–7.
5. Runge VM, Biswas J, Wintersperger BJ, Baumann SS, Jackson CB, Herborn CU, et al. The efficacy of gadobenate dimeglumine (Gd-BOPTA) at 3 Tesla in brain magnetic resonance imaging: comparison to 1.5

Tesla and a standard gadolinium chelate using a rat brain tumor model. Invest Radiol 2006;41:244–8.
6. Chappell PM, Pelc NJ, Foo TK, Glover GH, Haros SP, Enzmann DR. Comparison of lesion enhancement on spin-echo and gradient-echo images. Am J Neuroradiol 1994;15:37–44.
7. Rand S, Maravilla KR, Schmiedl U. Lesion enhancement in radio-frequency spoiled gradient-echo imaging: theory, experimental evaluation, and clinical implications. Am J Neuroradiol 1994;15:27–35.
8. Pui MH, Fok EC. MR imaging of the brain: comparison of gradient-echo and spin-echo pulse sequences. Am J Roentgenol 1995;165:959–62.
9. Fellner F, Holl K, Held P, Fellner C, Schmitt R, Bohm-Jurkovic H. A T1-weighted rapid three-dimensional gradient-echo technique (MP-RAGE) in preoperative MRI of intracranial tumours. Neuroradiology 1996;38: 199–206.
10. Li D, Haacke EM, Tarr RW, Venkatesan R, Lin W, Wielopolski P. Magnetic resonance imaging of the brain with gadopentetate dimeglumine-DTPA: comparison of T1-weighted spin-echo and 3D gradient-echo sequences. J Magn Reson Imaging 1996;6:415–24.
11. Elster AD. How much contrast is enough? Dependence of enhancement on field strength and MR pulse sequence. Eur Radiol 1997;7 Suppl 5:276–80.
12. Fischbach F, Bruhn H, Pech M, Neumann F, Ricke J, Felix R, et al. Efficacy of contrast medium use for neuroimaging at 3.0 T: utility of IR-FSE compared to other T1-weighted pulse sequences. J Comput Assist Tomogr 2005;29:499–505.
13. Raila FA, Bowles AP Jr, Perkins E, Terrell A. Sequential imaging and volumetric analysis of an intracerebral C6 glioma by means of a clinical MRI system. J Neurooncol 1999;43:11–7.
14. Thorsen F, Ersland L, Nordli H, Enger PO, Huszthy PC, Lundervold A, et al. Imaging of experimental rat gliomas using a clinical MR scanner. J Neurooncol 2003;63:225–31.
15. Blanchard J, Mathieu D, Patenaude Y, Fortin D. MR-pathological comparison in F98-Fischer glioma model using a human gantry. Can J Neurol Sci 2006;33: 86–91.
16. Wansapura JP, Holland SK, Dunn RS, Ball WS Jr. NMR relaxation times in the human brain at 3.0 tesla. J Magn Reson Imaging 1999;9:531–8.

Acta Radiologica rad134548.3d 23/10/07 20:33:45
The Charlesworth Group, Wakefield +44(0)1924 369598 - Rev 7.51n/W (Jan 20 2003)

262880